New Cubic Phase of Li$_3$N: Stability of the N^{3-} Ion to 200 GPa

A. Lazicki,[1,2] B. Maddox,[1,2] W. J. Evans,[1] C.-S Yoo,[1] A. K. McMahan,[1] W. E. Pickett,[2] R. T. Scalettar,[2]
M. Y. Hu,[3] and P. Chow[3]

[1]*Lawrence Livermore National Laboratory, Livermore, California 94550, USA*
[2]*Physics Department, University of California, Davis, California 95616, USA*
[3]*HPCAT/APS, Argonne National Laboratory, Argonne, Illinois 60439, USA*
(Received 29 April 2005; published 14 October 2005)

Diamond-anvil cell experiments augmented by first-principles calculations have found a remarkable stability of the N^{3-} ion in Li$_3$N to a sixfold volume reduction. A new (γ) phase is discovered above $40(\pm 5)$ GPa, with an 8% volume collapse and a band gap quadrupling at the transition determined by synchrotron x-ray diffraction and inelastic x-ray scattering. γ-Li$_3$N ($Fm3m$, Li$_3$Bi-like structure) remains stable up to 200 GPa, and calculations do not predict metallization until ~8 TPa. The high structural stability, wide band gap, and simple electronic structure make this N^{3-} based system analogous to lower valency compounds (MgO, NaCl, Ne), meriting its use as an internal pressure standard.

Nitrogen can form compounds with elements from almost every column in the periodic table, with chemical bonding ranging from covalent to ionic to metallic. Lithium nitride is the only known thermodynamically stable alkali metal nitride and is one of the most ionic of all known nitrides. At ambient pressure, the nitrogen exists in an anomalous multiply charged (N^{3-}) state [1,2] which is stable only because of its crystal environment—a hexagonal bipyramid of Li$^+$ ions. This layered structure (α-Li$_3$N, $P6/mmm$) consists of Li$_2$N layers, widely separated and connected by one lithium atom per unit cell occupying a site between the nitrogen atoms in adjacent layers [3,4]. This material is a superionic conductor via vacancy-induced Li$^+$ diffusion within the Li$_2$N layers [5–7]. Its potential for use as an electrolyte in lithium batteries [4], a hydrogen storage medium [8–11], and a component in the synthesis of GaN [12] has prompted several studies including an investigation into its behavior at high pressure [13].

At ~0.5 GPa, α-Li$_3$N transforms into a second layered hexagonal structure (β, $P6_3/mmc$) with BN-like honeycomb LiN layers [14]. In this structure, each nitrogen binds an additional lithium atom above and below the plane and, unlike the Li$_2$N layers in α-Li$_3$N, adjacent LiN layers are shifted relative to one another. β-Li$_3$N is metastable at ambient pressure and is typically found mixed with the α phase. It remains stable up to 35 GPa—the high-pressure limit of experiments on Li$_3$N to date. A second phase transition to a cubic structure—$P\bar{4}3m$ at 37.9 GPa [13] or $Fm3m$ at 27.6 GPa [15]—has been predicted. If it exists, the similarity of this phase to those of other simple ionic cubic solids such as NaCl makes it an interesting study, particularly in light of its higher ionicity. Understanding the behavior of the unstable and highly charged N^{3-} ions under large compression is of particular interest.

In this Letter, we present the first concrete experimental evidence that β-Li$_3$N indeed transforms to a cubic structure (γ-Li$_3$N) in the pressure range of 36–45 GPa. This

transformation represents an increase in structural and bonding strength and isotropy, and is accompanied by a relatively large volume collapse and a fourfold widening of the electronic band gap. γ-Li$_3$N is uncommonly stable and quite compressible in this pressure regime and up to at least 200 GPa, making it a good candidate for an internal pressure standard.

Polycrystalline lithium nitride powder (99.5% purity, CERAC, Inc.) was loaded into a membrane diamond-anvil cell of Lawrence Livermore National Laboratory (LLNL) design. Several diamond sizes were used to obtain an extended range of pressure up to 200 GPa. In the lower pressure experiments, argon was used as a pressure medium and internal pressure standard. For the high-pressure experiments, no pressure medium was used, and copper or ruby (Al$_2$O$_3$:Cr^{3+}) were included in the sample chamber as pressure indicators. Under nonhydrostatic conditions, the equation of state fitting parameters differed from those obtained under quasihydrostatic conditions by 8.7%, 0.8% and 13% for B_0, V_0 and B'_0, respectively. Samples were loaded in an argon environment as Li$_3$N is hygroscopic. High-pressure behavior was investigated by angle-dispersive powder x-ray diffraction (ADXD) at 16IDB and x-ray Raman scattering (XRS) at 16IDD of the High-Pressure Collaborative Access Team (HPCAT) beam lines at the Advanced Photon Source (APS). For the ADXD experiments, we used intense monochromatic x-rays ($\lambda =$ 0.3683 or 0.4126 Å) microfocused to ~10 μm at the sample using a pair of piezocrystal controlled bimorphic mirrors. X-ray diffraction patterns were recorded on a high-resolution image plate detector (MAR 350) and analyzed with the FIT2D, XRDA, and GSAS programs. For the XRS experiments, we used monochromatic x rays (9.687 keV) focused to ~20×50 μm at the sample through an x-ray translucent Be gasket by a pair of 1 m-long Kirkpatrick-Baez focusing mirrors. Six spherically bent Si(660) single crystal analyzers (50 mm in diameter) were vertically mounted on a 870 mm Rowland circle to

refocus inelastically scattered x-ray photons onto a Si detector (Amp Tek) at a scattering angle of 25° in a nearly back scattering geometry (Bragg angle of 88.6°). This configuration corresponds to a momentum transfer of $q \sim$ 2.2 Å^{-1}. The overall system provides an energy resolution of ~ 1 eV.

At low pressures our x-ray data indicate a coexistence of the α and β phases, consistent with previous observations [13]. The mixture converts to single phase (opaque) β-Li$_3$N near 0.5 GPa. Between 35 and 45 GPa, we observed β-phase transform to a new transparent phase, γ-Li$_3$N, which remains stable up to 201 GPa, the maximum pressure achieved in the present study. A possible beginning of this transition was reported in [13,14]. An additional transition to an orthorhombic structure predicted at 168 GPa [15] is not seen. Figure 1 shows the measured and refined diffraction patterns of γ-Li$_3$N at 43 and 201 GPa. The refinement was performed based on the Li$_3$Bi structure ($Fm3m$) with one formula unit per primitive fcc cell consisting of one lithium and one nitrogen ion occupying $m\bar{3}m$ sites, and the two additional lithium ions in the $\bar{4}3m$ sites, each tetrahedrally coordinated with 4 nitrogen ions. Slight changes in relative intensities of the diffraction peaks appear to be due to increasing occupancy of the Li $\bar{4}3m$ sites with pressure (92.2% at 43 GPa and 99.9% at 201 GPa).

The pressure-volume data for the β and γ phases and their third-order Birch-Murnaghan equation of state (BM-EOS) fits are shown in Fig. 2, with fitting parameters summarized in Table I. The $\beta \rightarrow \gamma$ transition is accompanied by an 8% volume collapse and an increase in the coordination number for every atom. In the β phase ($a \sim$ 3.20 Å, $c \sim 5.71$ Å, at the transition), each N^{3-} ion is surrounded by 11 Li$^+$ ions (three in the hexagonal planes at 1.85 Å, two above and below the plane at 1.90 Å, and six in trigonal prismatic coordination at 2.1 Å). In the γ phase

($a \sim 4.5$ Å), 14 Li$^+$ ions surround N^{3-}, eight tetrahedrally coordinated with N at 1.95 Å, and six octahedrally at 2.25 Å. Across the phase transition there is no discontinuity in the nearest-neighbor N distance (~ 3.23 Å), and the nearest N-Li distance even increases slightly. The significant increase in packing without a decrease in distance between highly charged N ions makes the γ phase highly preferred at high pressures. The more populated and symmetric distribution of Li ions serves to effectively shield the highly charged N ions from one another and even potentially to compress their ionic radii [16], stabilizing the cubic structure up to very large lattice constant reduction.

The compressibility of γ-Li$_3$N rivals other common and highly compressible closed-shell cubic solids [17,18] as seen in the inset of Fig. 2. The results clearly show that γ-Li$_3$N is harder than neon, but softer than MgO and even NaCl above 100 GPa. The distinct lack of broadening in the measured ADXD (seen at 201 GPa in Fig. 1) even in the absence of a pressure medium also suggests that this material has very low shear strength, which is consistent with a high compressibility. The similar trend in compressibility between γ-Li$_3$N and the isoelectronic close-shelled Ne appears analogous to the case of ionic CsI and Xe which follow nearly identical compression curves [19]. But unlike CsI and Xe, which undergo a whole series of high-pressure phase transitions, γ-Li$_3$N and Ne have a very high phase stability.

The differences in crystal structure of γ-Li$_3$N from the α and β phases suggest that there will also be distinct differences in electronic structure. To validate this conjecture, we have carried out XRS experiments at the nitrogen K absorption edge. The most distinctive features of this spectrum (Fig. 3) are a "near edge" peak near 397 eV and a separate broader band near 403 eV, both of which change with pressure. The relative intensity of the lower energy
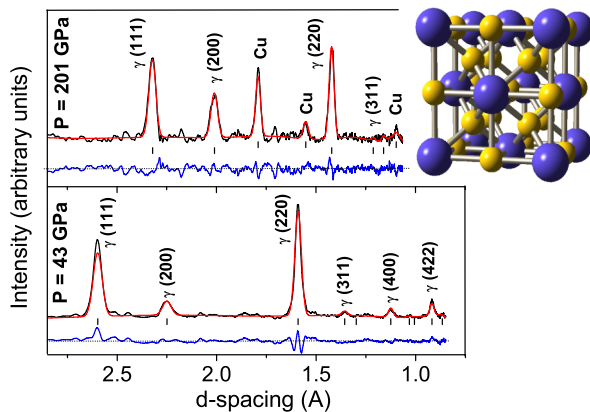

FIG. 1 (color online). ADXD diagrams of γ-Li$_3$N at 43 and 201 GPa, with refined and difference patterns. Miller indices are based on the cubic ($Fm3m$) structure shown, with large atoms representing the highly negative nitrogen ions, small representing lithium.

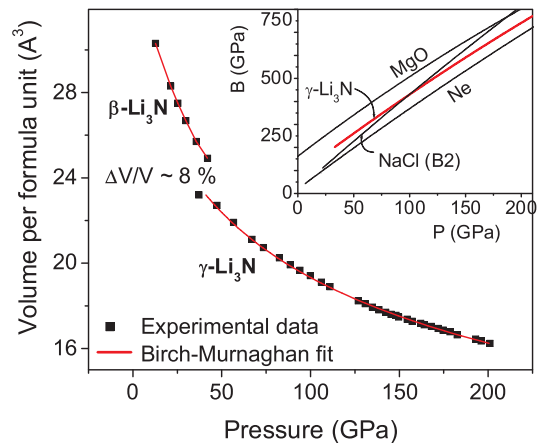FIG. 2 (color online). Equation of state of β- and γ-Li$_3$N. In the inset, the high-pressure bulk modulus of γ-Li$_3$N is compared to other common highly compressible materials [17,18]. (Curves are interpolated up to 200 GPa).

TABLE I.   Volume V_0 (values per formula unit), bulk modulus B_0, its pressure derivative B_0', volume change at the $\beta \rightarrow \gamma$ transition, and transition pressure as obtained in experimental and theoretical work in present and other studies. Experimental errors are primarily a result of nonhydrostaticity in the diamond-anvil cell. The γ phase predicted in Ref. [13] is space group $P\bar{4}3m$.

		V_0 (Å³)	B_0 (GPa)	B_0	$\frac{\Delta V}{V_0}$	P (GPa)
Experimental[a]	β	34.4(.8)	71(19)	3.9(.9)	8(2)%	40(5)
	γ	30.8(.8)	78(13)	4.2(.2)		
Theoretical	β	34.44(.08)	68(3)	3.6(.1)	6.7%	40.4
	γ	31.16(.08)	73.1(.8)	3.85(.01)		
[13][a]	β	35.04	74(6)	3.7(.7)		>35
[13]	β	30.88	78.2	3.77	8%	37.9
	γ	28.08	82.8	3.84		
[15]	β	33.36				28(5)
	γ	30.44				
[14][a]	β	34.48				>10

[a]Experimental results.

peak decreases from the α to the β phase and vanishes in the cubic and more closely packed γ phase. All peaks shift to higher energy with increasing pressure.

In order to explain the observed structural and spectral changes, we have performed first-principles electronic structure calculations. Because of the large sixfold compression carried out in these calculations, we used two methods for comparison: full-potential linearized augmented plane-waves as implemented in WIEN2K code [20] within the generalized gradient approximation [21] and a full-potential nonorthogonal local-orbital minimum basis band structure scheme [22], within the local spin-density approximation [23]. We found good agreement between these two results. Figure 4 summarizes total energy calculations on the β and γ phases at various com-
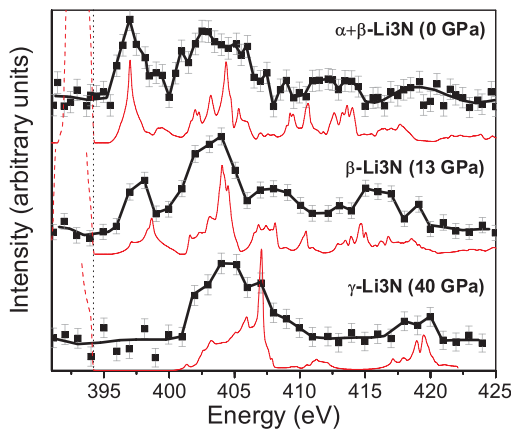
pressions and their BM-EOS fits (lines). The calculated equilibrium volumes, bulk moduli, and transition pressure are all in good agreement with experimental values (see Table I), giving us confidence in the theoretical models employed.

Using this model, we have calculated the projected nitrogen p density of states (pDOS) to compare with the XRS data (Fig. 3). A linear shift in energy (the same in each phase) is applied to the pDOS to align the leading edge peak with experiment. Within the dipole approximation, the relative intensities of the XRS spectrum are proportional to the pDOS and the squared dipole transition-matrix element. If the matrix element does not have a sharp energy dependence, the XRS and pDOS should be rather closely related, which is clearly seen in Fig. 3. This agreement reveals that the electronic states observed in the XRS study can be well understood as $1s \rightarrow 2p/3p$ transitions, and that core-hole-electron interactions (excitons) have a lesser effect on these spectra than often observed [24–26].

While the change from the α to the β phase is relatively small (and accounted for by the calculations), the change upon entering the γ phase is dramatic, and is a direct confirmation of the quadrupling of the band gap ($\sim$1.3 to $\sim$5.3 eV) predicted in the calculation at the transition. This gap increase is also evident in the optical change from the opaque β to the transparent γ phase. In spite of a similarity between this transition and the $1s$ to π^* and σ^* transitions in graphite-diamond and boron nitride, an examination of the p_x, p_y, and p_z character in Li$_3$N reveals that the near edge peak has a significant $p_{x,y}$ component in addition to p_z, and the main peak composition (primarily Li and N p character) does not suggest any significant hybridization between Li s and N p orbitals as is the case between B s and N p states in the largely covalently bonded BN. In ionic materials the band gap conventionally is a good measure of the degree of ionicity; the implication then is
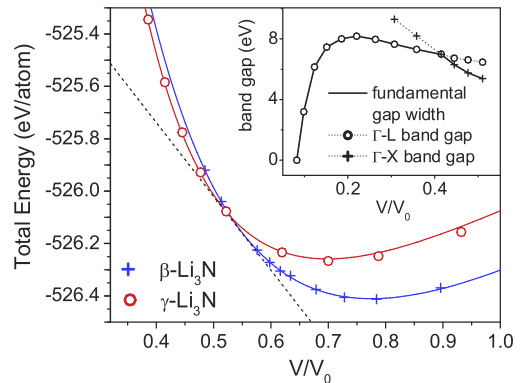

FIG. 3 (color online).   XRS of α-, β-, and γ-Li$_3$N shown in black, and error bars estimated as the square root of the counts. Nitrogen $2p$ projected DOS are shown in red (grey) beneath experimental curves, offset by 394.2 eV with occupied valence states as dashed lines, and vertical line representing the Fermi energy.

FIG. 4 (color online).   Calculated EOS of β- and γ-Li$_3$N. The slope of the dotted line represents the transition pressure. The collapse of the electronic band gap under pressure is shown in the inset. V_0 refers to the volume at ambient pressure in the α phase.

that in this regime pressure is not moving the system toward a covalent or metallic system (the typical behavior as bands broaden) but instead into a *much more strongly ionic* state. In the cubic phase, then, we expect more localized and symmetric charge distributions around the nitrogen atoms, making them even closer to the ideal N^{3-} state and explaining the insulating character and high stability of this phase. This transition is facilitated by the change from a layered structure to a cubic, well packed arrangement of ions. Further detailed analysis of the electronic structure will be provided elsewhere.

Our calculated electronic structures further reveal that, upon decreasing unit cell volume, the (indirect) band gap continues to increase up to a calculated pressure of ~ 760 GPa ($V/V_0 = 0.22$) before beginning to decrease (see Fig. 4, inset). Assuming no further phase transitions, band gap closure does not occur until ~ 8 TPa ($V/V_0 = 0.08$), which will be a lower limit because of the tendency of the local density approximation to underestimate the band gap. This high metallization pressure places γ-Li_3N in the same family as other closed-shell, cubic insulating solids such as Ne, MgO, and NaCl, which are predicted to metallize near 134, 21, and 0.5 TPa, respectively [27–29]. An examination of metallization in these materials reveals a trend that the states with smaller ℓ (orbital character) increase in energy with respect to larger ℓ because they are more extended and hence more greatly affected by pressure, so metallization occurs as a result of overlap between valence sp states and conduction d states [30]. Neon is isoelectronic to N^{3-}, and its metallization pressure is remarkably high because there is no $2d$ band, so that the overlap must occur between $2sp$ valence states and the much higher energy $3d$ conduction states. Li_3N is more complex, however, as the low-lying conduction bands have primarily $Li(2p)$ character, with a negligibly small amount of N d character at band closure. Therefore, the phenomenon in Li_3N is more of an interspecies metallization which perhaps explains its lower metallization pressure than predicted for the intraspecies metallization in neon.

In summary, we have provided the first coherent picture of the structural and electronic changes associated with a graphite-diamond–like transition in Li_3N. The high-pressure cubic phase has been discovered to possess several interesting and unique properties including unusually high phase stability and robust ionicity to pressures exceeding 200 GPa, high compressibility rivaling commonly used pressure media such as NaCl, and also an ultrahigh metallization pressure that makes it one of the most difficult materials to metallize that we know of.

[1] G. Kerker, Phys. Rev. B **23**, 6312 (1981).
[2] R. Dovesi *et al.*, Phys. Rev. B **30**, 972 (1984).
[3] E. Zintl and G. Brauer, Z. Elektrochem. Angew. Phys. Chem. **41**, 102 (1935).
[4] A. Rabenau and H. Schulz, J. Less Common Metals **50**, 155 (1976); A. Rabenau, Solid State Ionics **6**, 277 (1982).
[5] M. L. Wolf, J. Phys. C **17**, L285 (1984).
[6] J. Sarnthein *et al.*, Phys. Rev. B **53**, 9084 (1996).
[7] E. Bechtold-Schweickert *et al.*, Phys. Rev. B **30**, 2891 (1984).
[8] P. Chen *et al.*, Nature (London) **420**, 302 (2002).
[9] T. Ichikawa *et al.*, J. Alloys Compd. **365**, 271 (2004).
[10] Y. H. Hu *et al.*, Ind. Eng. Chem. Res. **44**, 1510 (2005).
[11] Y. Nakamori *et al.*, Appl. Phys. A: Mater. Sci. Process. **80**, 1 (2005).
[12] Y. Xie *et al.*, Science **272**, 1926 (1996).
[13] A. C. Ho *et al.*, Phys. Rev. B **59**, 6083 (1999).
[14] H. J. Beister *et al.*, Angew. Chem., Int. Ed. Engl. **27**, 1101 (1988).
[15] J. C. Schön *et al.*, J. Mater. Chem. **11**, 69 (2001).
[16] M. W. Wilson *et al.*, J. Chem. Phys. **104**, 8068 (1996).
[17] N. Sata *et al.*, Phys. Rev. B **65**, 104114 (2002).
[18] R. J. Hemley *et al.*, Phys. Rev. B **39**, 11 820 (1989).
[19] A. N. Zisman, I. V. Aleksandrov, and S. M. Stishov, Phys. Rev. B **32**, 484 (1985).
[20] P. Blaha *et al.*, WIEN2K, Karlheinz Schwarz, Technische Universität Wien, Wien, 2001.
[21] J. P. Perdew, K. Burke, and M. Ernzerhof, Phys. Rev. Lett. **77**, 3865 (1996).
[22] K. Koepernik and H. Eschrig, Phys. Rev. B **59**, 1743 (1999).
[23] J. P. Perdew and Y. Wang, Phys. Rev. B **45**, 13 244 (1992).
[24] R. Buczko *et al.*, Phys. Rev. Lett. **85**, 2168 (2000).
[25] J. A. Soininen, "*Final-State Interactions in Inelastic X-ray Scattering*," University of Helsinki, 2001.
[26] E. L. Shirley, Phys. Rev. Lett. **80**, 794 (1998); E. L. Shirley *et al.*, J. Electron Spectrosc. Relat. Phenom. **114–116**, 939 (2001).
[27] J. C. Boettger, Phys. Rev. B **33**, 6788 (1986).
[28] A. R. Oganov, M. J. Gillan, and G. D. Price, J. Chem. Phys. **118**, 10 174 (2003).
[29] J. L. Feldman *et al.*, Phys. Rev. B **42**, 2752 (1990).
[30] A. K. McMahan, Physica B&C (Amsterdam) **139–140**, 31 (1986); A. K. McMahan and R. C. Albers, Phys. Rev. Lett. **49**, 1198 (1982).